Available online at www.sciencedirect.com
SCIENCE DIRECT®
Dyes and Pigments 58 (2003) 227–237
DYES and PIGMENTS
www.elsevier.com/locate/dyepig

Synthesis, spectroscopic and electrochemical investigation of some new stilbazolium dyes

Amaresh Mishra[a,*], George R. Newkome[a], Charles N. Moorefield[a], Luis A. Godínez[b]

[a]*Center for Molecular Design and Recognition, Departments of Polymer Science and Chemistry, The University of Akron, Akron, OH 44325-4717, USA*

[b]*Centro de Investigación y Desarrollo Tecnológico en Electroquímica S.C., Apdo. Postal 064, C.P. 76700, Pedro Escobedo, Querétaro, Mexico*

Received 31 January 2003; received in revised form 7 March 2003; accepted 5 April 2003

Abstract

The synthesis of some new solvatochromic mono-, *bis*-, and tetra*kis*tilbazolium dyes, **2–5**, is presented. The dyes were characterized by ^{1}H, ^{13}C NMR and mass spectroscopy. The UV–vis spectroscopic investigation of these compounds shows broad absorption bands [assigned to intramolecular charge transfer (ICT) processes] in different solvents in the range of 450–520 nm. The electrochemical behavior of the dyes, on the other hand, showed an irreversible reduction voltammetric wave that was postulated to arise from the formation of a chemically reactive neutral radical species. From the simulation of cyclic voltammetry measurements at different scan rates, it was possible to compute thermodynamic potentials, electron transfer rate constants, and diffusion coefficients for all the compounds under study.

Keywords: Stilbazolium (hemicyanine) dyes; Denotritic; Absorption spectra; Hydrogen bonding; Electrochemical rate constant; Diffusion coefficient

1. Introduction

Cyanines are a class of dyes whose chemical structure is characterized by two nitrogen atoms (one of which is positively charged), which are separated by a conjugated bridge formed by a carbon framework. The importance of these dyes stems from their wide use in industries for many years as spectral sensitizers for silver halide photography, in optical disks as recording media, as photorefractive materials, in laser devices and even as anti-tumor reagents [1]. In order to understand in detail their photochemical and photophysical properties, the synthesis, based on a donor-acceptor design concept, and characterization of a large number of new cyanine dyes have been reported [1,2]. In this way, the systematic, spectroscopic, and electrochemical study of different dye molecules as a function of the variation of the nature of the donor and/or acceptor moieties,

* Corresponding author. Present address: Department of Chemical Sciences, Tata Institute of Fundamental Research, Homi Bhabha Road, Colaba, Mumbai, 400 005, India. Fax: +91 22 2215 2110/2181.
E-mail address: amishra@tifr.res.in (A. Mishra).

0143-7208/03/$ - see front matter © 2003 Elsevier Ltd. All rights reserved.
doi:10.1016/S0143-7208(03)00066-4

as well as the distance between them, has been used to achieve an improved understanding of charge transfer and sensitization processes of these molecules [1–3]. Related studies on cyanine dyes include self-aggregation phenomena [4,5], their use as fluorescent polarity probes [6–8], non linear optical [9,10], and electroactive materials [11,12]. Herein, we report the synthesis of a new series of solvatochromic mono-, *bis*-, and tetra*kis*styrylpyridinium dyes **2**–**5** (Fig. 1) along with their related spectroscopic and electrochemical properties.

2. Results and discussion

2.1. Synthesis

For purposes of comparison, 4′-(*N,N*′-dimethylaminostyryl)-*N*-pentyl pyridinium bromide (**1**) was prepared following a method reported in the literature [7,13]. Dye **2**, however, was accessed by coupling bromooctanoic acid with γ-picoline, which was then condensed with *N,N*-dimethylaminobenzaldehyde to afford the desired product,

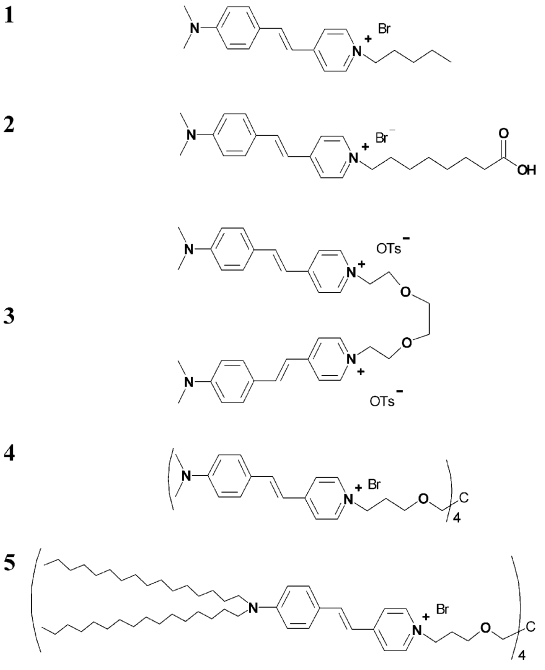

Fig. 1. Key structure of the dyes used in this study.

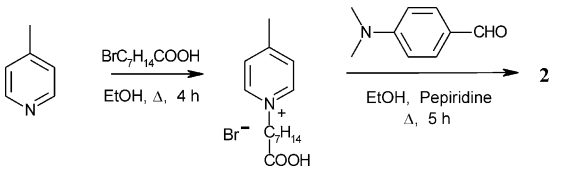

Scheme 1.

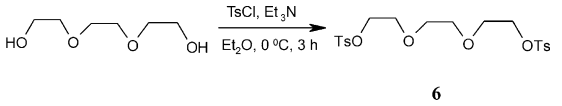

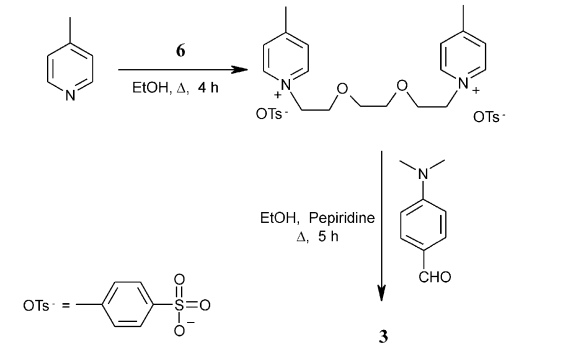

Scheme 2.

as red solid (Scheme 1). The tosylate derivative (**6**) of triethylene glycol was prepared (Scheme 2) by reaction with *p*-toluenesulfonyl chloride in presence of Et_3N, which was confirmed (^{13}C NMR) by the appearance of new peaks assigned to the tosylate group at 21.8 and 128–146 ppm region and the shift of the α-carbon of the hydroxyl group from 61.1 to 68.9 ppm. The tosylate **6** was then treated with γ-picoline and subsequently with *N,N*-dimethylaminobenzaldehyde to obtain dye **3**, as red solid; confirmation was by NMR and mass spectral analysis (see Section 3). Conversion of tetramesylate **7** [14] to the corresponding tetrabromide **8** (NaBr, DMF) (Scheme 3) was monitored (^{13}C NMR) by observation of the loss of peaks at 37.06 and 66.49 ppm (CH_3 and OCH_2, respectively) and the peak (^1H NMR) at 2.94 ppm (CH_3), and the appearance of a new signal (^{13}C NMR) at 30.86 ppm (CH_2Br). The reaction of aniline with 1-bromohexadacane to then afforded *N,N*-dihexadecyl- aniline **9** as a white solid, and was characterized by the appearance of a peak

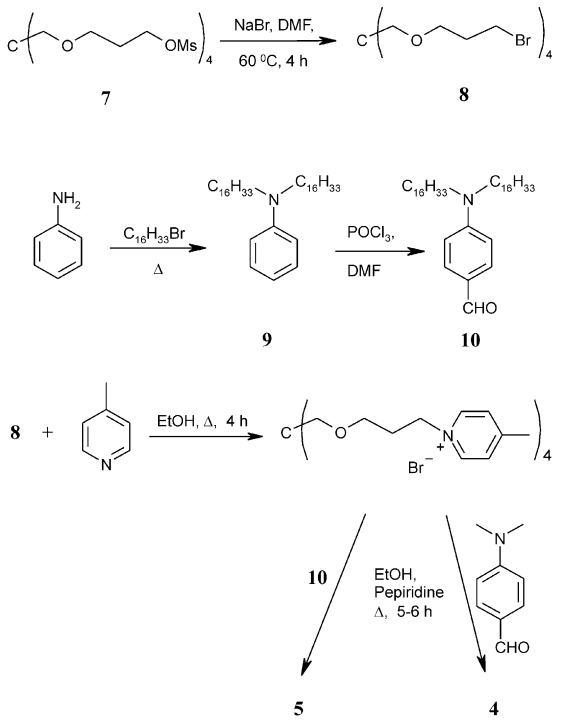

Scheme 3.

(^{13}C NMR) at 51.28 ppm for the N*C*H$_2$ carbon; formylation ($POCl_3$, DMF) then afforded **10**, as light brown solid. The successful synthesis of aldehyde **10** was confirmed (^{13}C NMR) by the appearance of a new resonance at 190.03 ppm and at 9.7 ppm (^{1}H NMR) assigned to the CHO group. This tetrabromide core **8** was then treated with γ-picoline, and subsequently condensed with *N,N*-dimethyl aminobenzaldehyde and *N,N*-dihexadecylaminobenzaldehyde (**10**) to afford, respectively, the corresponding dyes **4** and **5**, as red solids (Scheme 3). Based on the large coupling constants (^{1}H NMR) observed for the olefinic protons ($J_{trans} = 16.0$, 13.25, 16.0, and 15.75 Hz for **2**, **3**, **4** and **5**, respectively), all dyes (**2**–**5**) were determined to be *trans* conformers [15].

2.2. Spectroscopic studies

UV–vis spectroscopic measurements of the push–pull type dyes (Fig. 2) show broad absorption bands in the range of 450–520 nm corresponding to the (S1←S0 state) $n-\pi^*$ transition

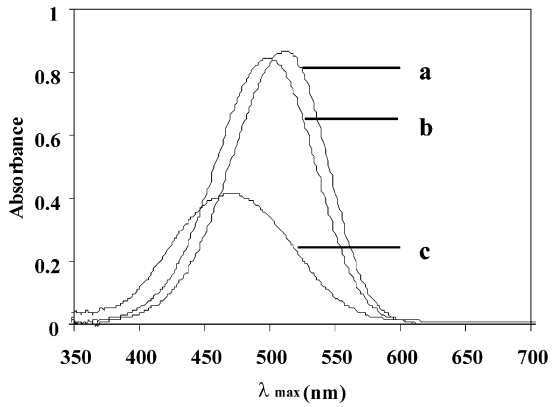

Fig. 2. Representative absorption spectra of dye **5** in various solvents. a: CH_2Cl_2, b: EtOH, c: H_2O respectively. [Dye] was maintained at 5 μM.

[15] attributed to an intramolecular charge transfer (ICT) involving the electron lone pair of the amino nitrogen and the cationic pyridinium nitrogen terminal [8]. Because of their strong charge transfer character, the absorption spectra are influenced by the medium polarity, as seen in solution phase (Fig. 2). In Table 1, for instance, the absorption spectral data of the five different dyes under study in various solvents are presented. A representative absorption spectrum of **1**–**5** in methanol is given in Fig. 3. It can be readily observed, that as the monochromophoric dyes **1** and **2** show λ_{max} at 450 nm in water, λ_{max} shifts to

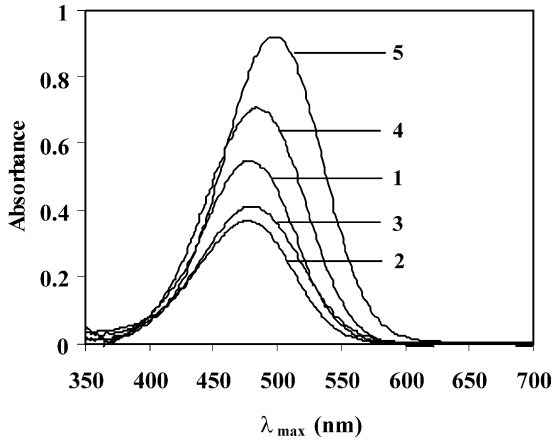

Fig. 3. Absorption spectra of dyes **1**–**5** in methanol. [Dye] was maintained at 20 μM for **1**, 10 μM for **2** and **3**, and 5 μM for **4** and **5**, respectively.

Table 1
Absorption spectral data (λ_{max} and log ε) of the styrylpyridinium dyes used in this study. The [dye] was maintained at 20 μM for **1**, 10 μM for **2** and **3**, and 5 μM for **4** and **5**, respectively

Solvents	α[a]	**1** λ_{max} (log ε)	**2** λ_{max} (log ε)	**3** λ_{max} (log ε)	**4** λ_{max} (log ε)	**5** λ_{max} (log ε)
Water	1.17	450(4.39)	450(4.33)	464(4.35)	468(4.67)	468(4.62)
MeOH	0.93	479(4.74)	477(4.57)	480(461)	486(4.85)	499(4.69)
EtOH	0.83	484(4.74)	481(4.56)	486(4.64)	484(4.92)	499(4.93)
i-Propanol	0.76	485(4.73)	480(4.58)	481(4.66)	481(4.9)	489(4.99)
$CHCl_3$	0.44	496(4.79)	496(4.54)	485(4.53)	484(4.89)	505(499)
CH_2Cl_2	0.3	513(479)	501(4.59)	499(4.63)	489(4.83)	511(4.94)

All measured solutions contained 1% MeOH.
[a] Acidity of solvent.

larger values as the number of chromophoric unit in the dye molecule increases.

It was also noted that as the solvent acidity (α) increases, a hypsochromic shift has been observed for the absorption spectra (Fig. 4) [16], indicating a specific hydrogen bonding interaction between dye and the solvent molecule [17,18]. Thus strong hydrogen bonding solvent forms hydrogen bond with the nitrogen lone pair of the dye molecule, which reduces the magnitude of the ICT interaction within the dye molecule and shows blue shift in absorption band [19]. The red shift in the absorption maxima of **5** in alcoholic solvents as compared to those for **1**–**4** (Table 1), on the other hand, may potentially be due to the presence of long alkyl chains, which in turn, should decrease the polarity in the surrounding microenvironment of the dye moiety and therefore the hydrogen bonding potential decreases between the dye and the solvent molecule.

2.3. Electrochemistry of dyes 1–5

The electrochemistry of dyes **1**–**5** was investigated in the cathodic region by carrying out cyclic voltammetry experiments on 1.0 mM solutions (except for **1** which was studied at a 0.5 mM concentration) of the relevant compound dissolved in deoxygenated 0.1 M of $TBAPF_6$ in anhydrous DMSO at room temperature. As can be readily seen in Fig. 5, the electrochemical response of the parent **2** is characterized by an irreversible peak that, according to published results on similar compounds, is due to the monoelectronic reduc-

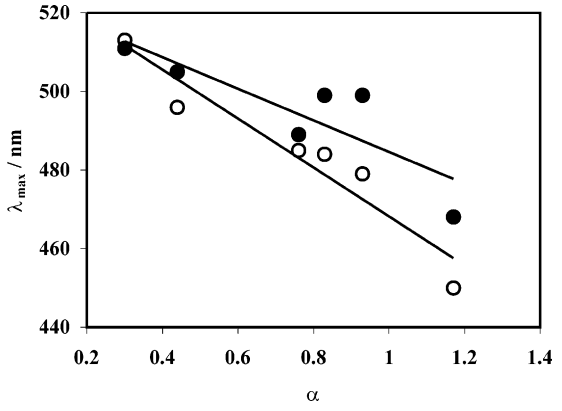

Fig. 4. Representative plot of the longest wavelength absorption maxima with solvent acidity (α) for compounds **1** (○) and **5** (●).

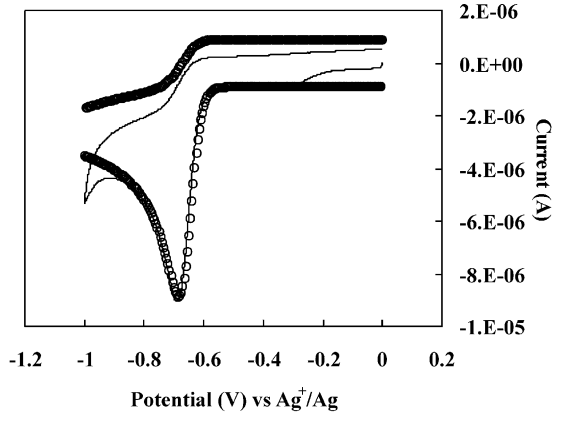

Fig. 5. Experimental (–) and simulated (○) CV responses of a 1.0 mM solution of **2** in $TBAPF_6$ 0.1 M in DMSO at 293 K. Scan rate 100 mV/s.

tion of the dye moiety [19,20]. As expected from the chemical structures of **1**–**5**, similar responses were observed for all the compounds under study, suggesting that the same type of electrochemical behavior characterizes the electro activity of the whole series. According to Lenhard and co-workers, the neutral radical formed upon reduction for this type of compounds is a very reactive species that readily undergoes a fast chemical dimerization reaction [20]. This chemical step gives rise to a non-electroactive compound which in turn, explains the absence of the corresponding anodic wave during the reverse scan [21].

Consistent with the voltammetric behavior of electrochemical–chemical mechanisms (EC) [22–25], CV experiments for **1**–**5** were conducted at different scan rates in the 20–800 mV/s range, and showed cathodic peak current and potential variations that allowed us to simulate the electrochemical response of the systems to obtain in this way the relevant electrochemical parameters (Redox potentials, E^{o}, electron transfer rate constants, k, and diffusion coefficients, D). Notably, these simulations employed specific assumptions.

First, the mechanism considered for the single-dye species **1** and **2** assumed a quasi-reversible electron transfer rate constant ($k_{1^+ \rightarrow 1}$ or $k_{2^+ \rightarrow 2}$), a very fast dimerization reaction and a large equilibrium constant (K_1 or K_2) for the formation of the non-electroactive compounds **11** and **12** [20].

$$\mathbf{1}^{+} + e^{-} \xrightarrow{E^{0}_{1^+/1'}, k_{1^+ \rightarrow 1}} \mathbf{1}^{\bullet}$$

$$\mathbf{1}^{\bullet} + \mathbf{1}^{\bullet} \overset{K_1}{\rightleftarrows} \mathbf{11}$$

$$\mathbf{2}^{+} + e^{-} \xrightarrow{E^{0}_{2^+/2'}, k_{2^+ \rightarrow 2}} \mathbf{2}^{\bullet}$$

$$\mathbf{2}^{\bullet} + \mathbf{2}^{\bullet} \overset{K_2}{\rightleftarrows} \mathbf{12}$$

On the other hand, the mechanism assumed for the multiple-chromophoric compounds **3**, **4** and **5**, also considered quasi-reversible electron transfer rate constants ($k_{i^{n+} \rightarrow i^{(n-1)+}}$), and fast dimerization rates, also characterized by large equilibrium constants (K_j) [21]. The structure of these compounds, however, led us to assume a slightly different mechanism from that proposed for **1** and **2**. In these cases dimerization was considered to occur *within* the electroactive molecule giving rise to the formation of the partially electroactive species $\mathbf{14}^{2+}$ and $\mathbf{16}^{2+}$ and to the non-electroactive species **13**. As can be seen in the following set of equations, compounds $\mathbf{14}^{2+}$ and $\mathbf{16}^{2+}$ keep reacting simultaneously at the electrode surface to form the completely non-electroactive compounds **15** and **17** [26].

$$\mathbf{3}^{2+} + e^{-} \xrightarrow{E^{0}_{3^{2+}/3^{+}}, k_{3^{2+} \rightarrow 3}} \mathbf{3}^{\bullet+}$$

$$\mathbf{3}^{\bullet+} + e^{-} \xrightarrow{E^{0}_{3^+/3'}, k_{3^+ \rightarrow 3}} \mathbf{3}^{\bullet\bullet}$$

$$\mathbf{3}^{\bullet\bullet} \overset{K_3}{\rightleftarrows} \mathbf{13}$$

$$\mathbf{4}^{4+} + e^{-} \xrightarrow{E^{0}_{4^{4+}/4^{3+}}, k_{4^{4+} \rightarrow 4^{3+}}} \mathbf{4}^{\bullet 3+}$$

$$\mathbf{4}^{\bullet 3+} + e^{-} \xrightarrow{E^{0}_{4^{3+}/4^{2+}}, k_{4^{3+} \rightarrow 4^{2+}}} \mathbf{4}^{\bullet\bullet 2+}$$

$$\mathbf{4}^{\bullet\bullet 2+} \overset{K_4}{\rightleftarrows} \mathbf{14}^{2+}$$

$$\mathbf{5}^{\bullet 3+} + e^{-} \xrightarrow{E^{0}_{5^{3+}/5^{3+}}, k_{5^{2+} \rightarrow 5^{2+}}} \mathbf{5}^{\bullet\bullet 2+}$$

$$\mathbf{5}^{4+} + e^{-} \xrightarrow{E^{0}_{5^{4+}/5^{3+}}, k_{5^{4+} \rightarrow 5^{3+}}} \mathbf{5}^{\bullet 3+}$$

$$\mathbf{5}^{\bullet\bullet 2+} \overset{K_5}{\rightleftarrows} \mathbf{16}^{2+}$$

$$\mathbf{14}^{2+} + e^{-} \xrightarrow{E^{0}_{9^{2+}/9^{+}}, k_{9^{2+} \rightarrow 9^{+}}} \mathbf{14}^{\bullet+}$$

$$\mathbf{14}^{\bullet+} + e^{-} \xrightarrow{E^{0}_{9^+/9^+}, k_{9^+ \rightarrow 9}} \mathbf{14}^{\bullet\bullet}$$

$$\mathbf{14}^{\bullet\bullet} \overset{K_9}{\rightleftarrows} \mathbf{15}$$

$$\mathbf{16}^{2+} + e^{-} \xrightarrow{E^{0}_{10^{2+}/10^{2+}}, k_{10^+ \rightarrow 10^+}} \mathbf{16}^{\bullet+}$$

$$\mathbf{16}^{\bullet+} + e^{-} \xrightarrow{E^{0}_{10^+/10'}, k_{10^+ \rightarrow 10}} \mathbf{16}^{\bullet\bullet}$$

$$\mathbf{16}^{\bullet\bullet} \overset{K_{10}}{\rightleftarrows} \mathbf{17}$$

The *intramolecular* dimerization mechanism of the multiple-redox center compounds **3**–**5**, was chosen over that of the *intermolecular* dimerization process in view of the increased availability of neutral radical units within compounds **3**, **4** or **5** as compared to that in the dilute solution.

In addition to the assumptions employed in the mechanisms just described, there is another approximation that had to be done in order to reduce the complexity of the data treatment for the heterogeneous reactions of the multiple redox-center species **3**–**5**. Although in these cases each one of the electron transfer steps must be characterized by a different electron transfer rate constant ($k_{i^{n+}\rightarrow i^{(n-1)+}}$), it was decided to use a single *average* value for compounds **3**–**5** so that the number of variables to be fitted could be reduced. As will be commented on later, this consideration results in k values for the multi-chromophoric compounds **3**–**5** that are not strictly meaningful when compared to those obtained for the single-dye species **1** and **2** but that nevertheless, constitute a rough approximation that reflect the average behavior of the relevant electroactive molecules.

In terms of the thermodynamic redox potentials for **3**–**5** in which multiple equivalent redox active centers are incorporated within the molecule, the absence of multiple reduction peaks in the CV responses suggests that the reduction energies can in principle be considered to be the same for each one of the dye moieties, i.e. the cyanine redox centers can be assumed to be non-interacting electroactive units [27]. As pointed out by Bard and co-workers however, [24,28,29] statistical criteria dictates that the difference between the formal potentials of the *m*th and the first electron transfer of m non-interacting electroactive sites in a molecule, can be formally described by the following relationship [24]:

$$E_m^0 - E_1^0 = -\left(\frac{2RT}{F}\right)\ln(m)$$

where T corresponds to temperature in Kelvin and R and F are the gas and Faraday constants respectively. Thus, in the case of the compounds under study, the consecutive formal potentials are separated by 34 mV for compound **3** and by 34, 20 and 14 mV for compounds **4** and **5**.

The simulations for the voltammograms experimentally obtained were conducted using the DIGISIM simulation program developed by M. Rudolph and commercialized by BAS inc. (West Layafette, Indiana, USA) [30]. As can be seen in Figs. 5 and 6, the simulated and experimental values for peak current and potentials are pretty close for dye **1**–**4** and relatively bad for the experiments carried out with **5**. Problems arising with adsorption of this compound on the surface of the electrode as well as a necessary change in

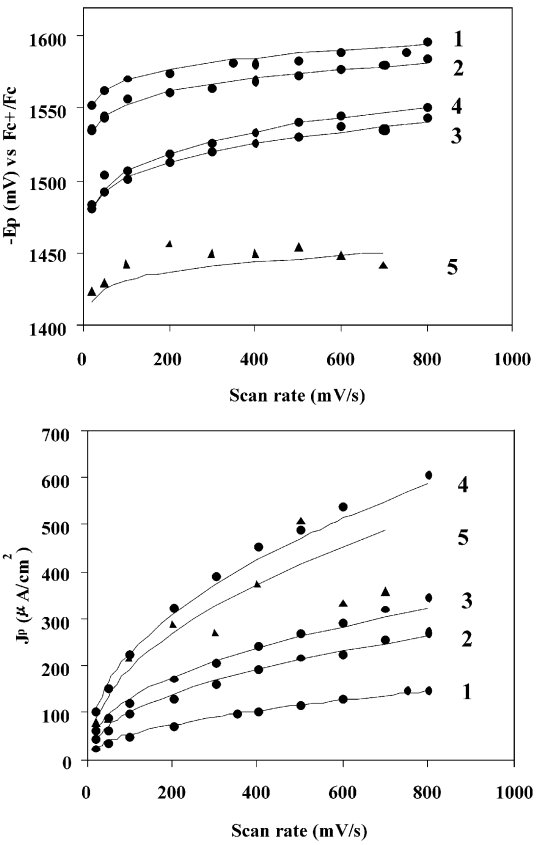

Fig. 6. Peak potential (E_p) and current density (J_p) dependence on scan rate for the CV responses of 0.5 mM and 1.0 mM solutions of dyes **1** and **2**–**5**, respectively. The continuous lines show the simulated behavior calculated with the values presented in Table 2 and the markers (●) and (▲) correspond to the experimental values obtained for compounds **1**–**4** and **5**, respectively.

the electrolytic medium due to solubility problems, made its study somewhat problematic.

Thus, as can be seen from the values presented in Table 2, the formal potential for the $\mathbf{2}^{+}/\mathbf{2}$ couple, −1.645 V vs. Fc^{+}/Fc, is the most negative of the series, implying that a larger amount of energy must be rendered to the dye in order to reduce it and form in this way the neutral radical species. Comparison of this value with that corresponding to the potential obtained for **1**, suggests that the terminal carboxylic acid group in **2** should be somehow stabilizing the positive charge of the dye moiety. Since the alkyl chain that characterizes the structure of compound **2** bears seven methylene groups, and the concentration of the electroactive compound in the voltammetric experiments is relatively low, we speculate that there must exist a folded form of compound **2** that, by means of a electrostatic interaction, should be responsible for the more negative reduction potential computed from our experimental data (see Fig. 7) [31].

The thermodynamic potentials for **3–5** on the other hand, clearly show more positive values when compared to those found for compounds **1** and **2**. This difference reflects a smaller energy requirement of **3**, **4**, and **5** to form the reduced neutral radical species during the reduction process. Since these three compounds bear multiple cationic redox active units within the electroactive molecule, it is possible to suggest that the intramolecular repulsive electrostatic interaction between the cationic dye units should result on a lack of stability that expresses itself as more positive reduction potential values. This explanation is also consistent with the fact that the potentials of **3**, which only has two cationic dye units and therefore experiences less repulsive interactions, are more negative than those of compounds **4** and **5** which, having four positive moieties, are characterized by stronger intramolecular repulsive interactions.

Table 2
Electrochemical parameters for compounds **1–5** obtained from the simulation of the CV experimental data at 293 K

Compound	E° (V) vs Fc^{+}/Fc	k_e (cm/s)	D (cm^2/s)
1	−1.568	8.5×10^{-2}	1.3×10^{-6}
2	−1.645	5.3×10^{-2}	1.2×10^{-6}
3	−1.474	3.3×10^{-3}	5.8×10^{-7}
	−1.508		
4	−1.421	2.5×10^{-3}	5.5×10^{-7}
	−1.455		
	−1.475		
	−1.489		
5	−1.414	3.0×10^{-2}	2.8×10^{-7}
	−1.448		
	−1.468		
	−1.482		

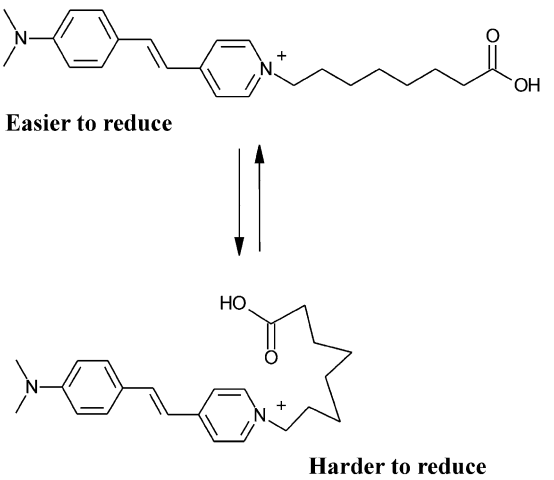

Fig. 7. Cartoon showing the proposed intramolecular interaction between the carboxylic and cyanine dye moieties in **2**.

In terms of the electron transfer rate constants obtained from the simulations, the data in Table 2 show that the values corresponding to **1** and **2** are roughly the same, and approximately 20 times larger than those corresponding to the average values obtained for the multiple-dyes **3** and **4**. As pointed out before, the rate constants reported for compounds **3** and **4** are actually *average* values that reflect the combined rates of the complex electron transfer events of the different electroactive moieties involved. Although a detailed interpretation of the nature of these values is not meaningful, it could be seen that as a rough approximation these compounds exchange electrons with the electrode surface in a clearly slower fashion when compared to the parent dyes **1** and **2**. With respect to dye **5**, and in comparison to the freely soluble dyes **3** and **4**, we speculate that the

hydrophobic alkyl chains that characterize the structure of the alkylated species **5** may be responsible for an adsorption phenomena at the graphite electrode surface that in turn, could modify the electron transfer kinetics in such a way that a relatively high average electron transfer rate constant is readily observed. This explanation is reasonable not only because the physical affinity of the alkyl chains in **5** and the graphite electrode surface can be easily expected, but also because its solubility in the modified electrolytic medium (50% CH_2Cl_2/DMSO, see section 3) was close to its limiting value. In any case, this point is very speculative and should be taken with caution. The fact that the medium is chemically different and that the reproducibility of the experiments was poor (probably also due to adsorption phenomena at the electrode surface), made the simulation carried out for **5** not a very successful experience and therefore the interpretation of the data should be taken just as a reasonable explanation.

The diffusion coefficients, on the other hand, seem to be in line for what it could be expected for this series of compounds. Inspection of the values presented in Table 2 for instance, shows that the largest diffusion coefficient values were obtained for compounds **1** and **2**. It is interesting to note however that these values are not only the largest of the series, but also very similar between each other, a fact that clearly supports the hypothesis of a folded stable isomer of **2** which, as has been previously discussed, must be assumed in order to explain the large negative redox potential computed for this compound (see Fig. 7). The diffusion coefficients for compounds **3**–**5** on the other hand, are substantially smaller than those found for species **1** and **2**, a fact that obviously reflects the larger size of the relevant compounds.

3. Experimental

3.1. General

All starting reagents and solvents (reagent grade) were purchased from Aldrich Chemical Co. and used without further purification. All melting points were taken in capillary tubes and are uncorrected. Column chromatography was conducted using basic alumina and silica gel (60–200 μm) from Fisher Scientific with the stipulated solvent mixture.

^1H and ^{13}C NMR spectra were recorded at 250 and 62 MHz, respectively, on a Bruker AC 250 MHz spectrometer. *J* values are given in Hz. Mass spectral data were obtained on an Esquire electro spray ionization (ESI-MS) and matrix assisted laser desorption ionization time-of-flight (MALDI-TOF) mass spectrometer.

Absorption spectra were recorded in a METSON UV–vis spectrophotometer. A concentration of (ca. 1 mM/L) stock solution was prepared separately for each dye by dissolving the required amount of the dye in MeOH. The solutions for spectral measurements were prepared by adding the appropriate amount of the dye to maintain its concentration at 20 μM for **1**, 10 μM for **2** and **3**, and 5 μM for **4** and **5**, respectively. All measured dye solutions contained 1% MeOH. Aliquots (3 ml) of these solutions were added to quartz cuvettes thermostated at 25 °C.

Cyclic voltammetry (CV) experiments at 20 °C were carried out using a BAS 100-W potensiostat coupled to C-3 cell stand and controlled by means of the BAS developed software loaded into a PC. The electrochemical experiments were conducted using a conventional three electrode standard setup 2 cm^3 cell (BAS, West Lyafette, IN) in which a glassy carbon disk electrode (3.2 mm diameter), a platinum wire and a Ag wire were properly fitted as the working, counter, and pseudo-reference electrodes, respectively. Before each experiment, the working solution (1.0 mM of the electroactive compound in 0.1 M of tetrabutylammonium hexafluorophosphate ($TBAPF_6$) in anhydrous dimethyl sulfoxide (DMSO)) was carefully deoxygenated by bubbling dry argon for at least 10 min. In the case of compound **5** however, a 50% solution of CH_2Cl_2/DMSO with the same supporting electrolyte was used due to solubility problems. In all cases, and before each potential scan was carried out, the working electrode was carefully polished in sequential steps with 0.05 μM alumina–water mixture and 0.25 μM particle size diamond polishing compound on a felt surface. Since the potential was followed through a pseudo-reference silver electrode, a second set of voltammograms

was obtained after adding a small amount of ferrocene to the solution. The reversible electrochemical signal of the ferrocene/ferrocinium couple did not interfere with the electrochemistry of any of the compounds under study and therefore allowed its use as a reference against which, the potentials reported in this work were measured.

3.2. Synthetic procedure

3.2.1. General Procedure for the synthesis of 4-(N,N-dimethylaminostyryl)pyridinium octanoic acid (2)

A mixture of 8-bromooctanoic acid (500 mg, 2.24 mmol) and γ-picoline (200 mg, 2.24 mmol) in EtOH (10 ml) was refluxed for 8 h. After cooling to 25 °C, the solvent was removed *in vacuo* giving a residue, which was washed with Et_2O to afford the γ-picolinium salt as white solid. Then *N,N*-dimethylaminobenzaldehyde (332 mg, 2.23 mmol) in EtOH (10 ml) and 2–3 drops of piperidine, as catalyst, were added to the salt and then this mixture was refluxed for 5 h. After cooling in an ice bath, the red solid was filtered and then crystallized from EtOH/hexane (70:30) to afford (70%) of the desired dye **2**, as red solid: 670 mg, mp 183–185 °C; δ_C (DMSO-d_6) 25.66, 28.54, 29.05, 30.83 (CH_2), 39.77 (NCH_3), 59.29 (NCH_2), 112.21, 117.45, 122.72, 122.81, 130.51, 142.42, 143.83, 152.15, 153.96 (C_{Ar}), 177.10 (CO_2H); δ_H (DMSO-d_6) 1.18 (6 H, s, CH_2), 1.44, 1.86, 2.03 (6 H, t, CH_2), 3.92 (6 H, s, CH_3), 4.45 (2 H, t, CH_2) 6.78 (2 H, d, *J* 8.6, ArH), 6.83 (4 H, d, *J* 16, ArH), 7.46 (8 H, d, *J* 8.6, ArH), 7.58 (4 H, d, *J* 16, ArH), 7.83 (8 H, d, *J* 6.3, ArH), 9.21 (8 H, d, *J* 6.3, ArH); ESI-MS *m/z* 367 $(M-Br)^+$ (calcd. $C_{23}H_{31}N_2O_2Br$; 447). Anal. calcd for $C_{23}H_{31}N_2O_2Br$: C, 61.74; H, 6.98; N, 6.26; found: C, 61.82; H, 6.93; N, 6.36.

3.2.2. 1,8-Di(tosyl) triethylene glycol (6)

To a stirred solution of triethylene glycol (1.5 g, 10 mmol) and Et_3N (2.12 g, 21 mmol) in dry Et_2O (20 ml) added dropwise tosyl chloride (3.99 g, 21 mmol) in Et_2O at 0 °C. After 1 h at 0 °C, then 3 h at 25 °C, the triethylammonium salt was filtered and the solvent was evaporated in vacuo to give the crude residue, which was dissolved in CH_2Cl_2 and then sequentially washed with $NaHCO_3$ (2×10 ml) and water (2×20 mL). The organic layer was dried (Na_2SO_4) and concentrated in vacuo to afford a solid, which was column chromatographed eluting with EtOAc/hexane mixture (2:1) to afford (85%) the desired **6**, as a white solid: 3.89 g; δ_C ($CDCl_3$) 21.80 (CH_3), 68.90, 69.39, 70.84 (CH_2), 128.12, 130.03, 133.13, 145.05 (C_{Ar}); δ_H ($CDCl_3$) 2.44 (6 H, s, CH_3), 3.52 (4 H, s, CH_2), 3.65 (4 H, t, CH_2), 4.14 (4 H, t, CH_2), 7.34 (4 H, d, *J* 6.75, ArH), 7.78 (4 H, d, J 6.75, ArH); ESI-MS *m/z* 481 $(M+Na)^+$, 497 $(M+K)^+$ (Calc. $C_{20}H_{26}O_8S_2$; 458).

3.2.3. Bis(N,N-dimethylaminostyrylpyridinium tosylate) possessing a TEG spacer (3)

Prepared (75%) by the above general procedure, using **6** (200 mg, 0.436 mmol), γ-picoline (80 mg, 0.873 mmol), and *N,N*-dimethylaminobenzaldehyde (128 mg, 0.873 mmol): 250 mg; mp 195–197 °C; δ_C (DMSO-d_6) 20.80 (CH_3), 39.69 (NCH_2), 58.65 (NCH_3), 68.83, 69.56 (CH_2O), 111.91, 117.02, 122.05, 122.45, 125.53, 128.15, 130.32, 137.78, 142.34, 143.87, 145.62, 151.93, 153.91 (C_{Ar}); δ_H (DMSO-d_6) 1.76 (12 H, s, CH_3); 2.99 (6 H, s, CH_3); 3.32 (8 H, t, CH_2) 4.07 (4 H, t, CH_2), 6.23 (4 H, d, *J* 7.25 ArH), 6.6 (4 H, d, *J* 6.75, ArH), 6.62 (2 H, d, *J* 13.25, ArH), 7.01 (4 H, d, *J* 6.75, ArH), 7.05 (4 H, d, *J* 7.25, ArH), 7.37 (2 H, d, *J* 13.25, ArH), 7.52 (4 H, d, *J* 5, ArH), 8.16 (4 H, d, *J* 5, ArH); ESI-MS *m/z* 282 $(M-2OTs)^{2+}$, 735.4 $(M-OTs)^+$ (calc. $C_{50}H_{58}N_4O_8S_2$; 907.16). Anal. calc. for $C_{50}H_{58}N_4O_8S_2$: C, 66.2; H, 6.44; N, 6.18; found: C, 66.08; H, 6.48; N, 6.24.

3.2.4. Tetrakis(5-bromo-2-oxapentyl)methane (8)

To a stirred solution of tetrakis(5-mesyloxy-2-oxabutyl)methane **7**, (3 g, 4.84 mmol) in DMF (20 ml), excess sodium bromide (3.99 g, 38 mmol) was added. The mixture was stirred at 60 °C for 4 h. After cooling, the mixture was filtered, evaporated in vacuo to give a solid, which was column chromatographed (SiO_2) eluting with an EtOAc:hexane mixture (1:1) to afford (95%) the desired tetrabromide **8**, as a colorless liquid: 2.85 g; δ_C ($CDCl_3$) 30.86 (CH_2Br), 32.83 ($CH_2CH_2CH_2$), 45.47 (^tC), 68.56 (CH_2O), 69.46 ($^tCCH_2$); δ_H ($CDCl_3$) 2.08 (8 H, q, CH_2); 3.37 (8 H, s, CH_2); 3.49 (8 H, t, CH_2) 3.50 (8 H, t, CH_2); MALDI TOF MS *m/z* 616.6 $(M+H)^+$ (calc. $C_{17}H_{32}Br_4O_4$; 616).

3.2.5. N,N-di(hexadecyl)aniline (9)

A mixture of aniline (1.02 g, 11 mmol) and an excess of 1-bromohexadecane (10.03 g, 33 mmol) was refluxed for 24 h. After cooling, the resulting ammonium salt was washed with NaOH solution, extracted with Et_2O, dried ($MgSO_4$), and evaporated in vacuo to give a crude product, which was column chromatographed eluting with hexane to afford (70%) **9**, as a white solid: 5.35 g; mp 48–50 °C. δ_C ($CDCl_3$) 14.36 (CH_3), 22.97 (CH_3CH_2), 27.48, 29.67, 29.85, 29.98, 32.22, (CH_2), 51.28 (NCH_2), 111.83, 115.29, 129.35, 148.31(C_{Ar}); δ_H (CDCl3) 1.0 (6 H, t, CH_3), 1.2–1.6 (52 H, br, s, CH_2), 1.68 (4 H, t, CH_2) 3.34 (4 H, t, CH_2), 6.71 (3 H, m, Ar*H*), 7.29 (2 H, t, ArH).

3.2.6. 4-[N,N-di(hexadecylamino)]benzaldehyde (10)

To a cooled (5 °C) solution of freshly distilled anhydrous DMF (15 g), was added $POCl_3$ (1.13 g, 7.39 mmol) within 5 min. The mixture was stirred for 30 min. Then 4-[*N,N*-di(hexadecyl)]aniline (**9**; 4 g, 7.39 mmol) was added to the solution and the resulting mixture was heated for 3 h at 80 °C. The mixture was hydrolyzed by a slow addition of ice-cold water and then neutralized with 5M NaOH. The precipitate was collected and recrystallized (EtOH/hexane) to afford (78%) the desired aldehyde **10**, as light brown solid: 3.28 g; m.p. 58 °C; δ_C ($CDCl_3$) 14.34 (CH_3), 22.88, 27.23, 27.31, 29.57, 29.65, 29.87, 32.12 (CH_2), 51.27 (NCH_2), 110.79, 124.64, 132.37, 152.72 (C_{Ar}), 190.03 (*C*HO); δ_H ($CDCl_3$) 0.88 (6 H, t, CH_3), 1.2–1.4 (52 H, br, s, CH_2), 1.61 (4 H, m, CH_2), 3.34 (4 H, t, CH_2), 6.64 (2 H, d, ArH) 7.7 (2*H*, d, ArH), 9.7 (1H, s, CHO); MALDI TOF MS *m*/*z* 570.5 $(M+H)^+$, 542 (M^+-CO), (calc. $C_{39}H_{71}NO$; 569.5).

3.2.7. Tetrakis(N,N-dimethylaminostyrylpyridinium bromide) (4)

Prepared (70%) by the General Procedure, using **8** (200 mg, 0.322 mmol), γ-picoline (120 mg, 1.29 mmol), and *N,N*-dimethylaminobenzaldehyde (192 mg, 1.29 mmol): 342 mg; mp 265–267 °C; δ_C (DMSO-d_6) 30.41 (CH_2CH_2), 44.40 (^tC), 57.03 (NCH_2), 67.87 (CH_2O), 69.47 ($^tCCH_2$), 111.85, 117.09, 112.25, 112.47, 130.23, 142.16, 143.56, 151.76, 153.69 (C_{Ar}); δ_H (DMSO-d_6) 1.62 (8 H, t, CH_2); 2.02 (8 H, s, CH_2); 2.56 (8 H, t, CH_2) 2.95 (24 H, s, CH_3) 4.03 (8 H, t, CH_2), 6.22 (8 H, d, *J* 8.5, ArH), 6.73 (4 H, d, *J* 16, ArH), 7.1 (8 H, d, *J* 8.5, ArH), 7.49 (4 H, d, *J* 16, ArH), 7.62 (8 H, d, *J* 5, ArH), 8.38 (8 H, d, *J* 5, ArH); ESI-MS *m*/*z* 299 $(M-4Br^-)^{4+}$, 425 $(M-3Br^-)^{3+}$, 678 $(M-2Br^-)^{2+}$, (calc. $C_{77}H_{96}N_8O_4Br_4$; 1517.3). Anal. calc. for $C_{77}H_{96}N_8O_4Br_4$: C, 60.95; H, 6.38; N, 7.38; found: C, 61.12; H, 6.41; N, 7.29.

3.2.8. Tetrakis(N,N-dihexadecylaminostyrylpyridinium bromide) (5)

Was prepared (65%) by the General Procedure, using **8** (200 mg, 0.322 mmol), γ-picoline (120 mg, 1.29 mmol), and **10** (734 mg, 1.29 mmol): 670 mg; mp 265–267 °C; δ_C ($CDCl_3$) 14.26 (CH_3), 22.81 (CH_3CH_2), 27.23, 27.43, 29.48, 29.63, 29.81, 31.8, 32.04 (CH_2), 45.38 (^tC), 51.22 (CH_2NCH_2), 57.69 (NCH_2), 68.24 (OCH_2), 69.80 ($^tCCH_2$), 111.64, 116.18, 121.76, 122.65, 131, 142.74, 144.06, 150.45, 154.11 (C_{Ar}); δ_H ($CDCl_3$) 0.81 (24 H, t, CH_3); 1.2 (aliphatic H, br, s); 1.53 (16 H, m, CH_2) 2.25 (8 H, m, CH_2) 3-3.4 (24 H, br, CH_2), 3.56 (8 H, t, CH_2), 4.79 (8 H, t, CH_2), 6.55 (8 H, d, *J* 8.5, ArH), 6.83 (4 H, d, *J* 15.75, ArH), 7.46 (8 H, d, *J* 8.5, ArH), 7.58 (4 H, d, *J* 15.75, ArH), 7.83 (8 H, d, *J* 6.3, ArH), 9.21 (8 H, d, *J* 6.3, ArH); ESI-MS *m*/*z* 987$(M-3Br^-)^{3+}$, 1520 $(M-2Br^-)^{2+}$, (calcd. $C_{197}H_{336}Br_4N_8O_4$; 3200.5). Anal. calcd for $C_{197}H_{336}N_8O_4Br_4$: C, 73.93; H, 10.58; N, 3.5; found: C, 74.17; H, 10.56; N, 3.56.

4. Conclusion

In the context of the potential and practical applications of the cyanine dyes, we have synthesized a new series of stilbazolium dyes and studied their physicochemical properties. These novel dyes show unique solvatochromic behaviour. Interactions with the electrode surface was demonstrated to depend upon the number of chromophoric units and the type of substituent present. Quasi-reversible electron transfer rates and fast dimerization reactions were observed for these dyes during electrochemical study. Dye **2** revealed a large cathodic shift due to the stabilization promoted by back-folding of terminal COOH group. With respect to

dyes **3**–**5**, in which multiple redox centers are present, only one redox peak was observed because of weak coupling among the electroactive units. It is expected that some of these dyes (e.g. **4** and **5**), could constitute the basis of a new group of dendritic materials that could find important applications in the field of non-linear optics, fluorescent probes, and biological studies.

Acknowledgements

We gratefully thank the National Science Foundation (DMR 0196231) and the Office of Naval Research (N00014-99-1-0082). L.A.G. whishes to express his gratitude to CONACyT (J-34905-E) and to the Mexican Academy of Sciences, the American Chemical Society, and Prof. George R. Newkome for financial support during a summer internship at the University of Akron. Helpful discussions with Y. Meas, R. Ortega and A. E. Kaifer are also gratefully acknowledged.

References

[1] Mishra A, Behera RK, Behera PK, Mishra BK, Behera GB. Chem Rev 2000;100:1973.
[2] Zhu Z. Dyes and Pigments 1995;27:77.
[3] De Silva AP, Gunaratne HQN, Bunnlaugsson T, Huxaley AJM, McCoy CP, Rademacher JT, Rice TE. Chem Rev 1997;97:1515.
[4] Mishra JK, Sahay AK, Mishra BK. Ind J Chem A 1991; 30:886.
[5] Harrison WJ, Mateer DL, Tiddy GJ. J Phys Chem 1996; 100:2310.
[6] Mishra A, Patel S, Behera RK, Mishra BK, Behera GB. Bull Chem Soc Jpn 1997;70:2913.
[7] Mishra A, Behera RK, Mishra BK, Behera GB. J Photochem and Photobiol A 1999;121:63.
[8] Mishra A, Behera GB, Krishna MMG, Periasamy N. J Luminescence 2001;92:175.
[9] Carpenter MA, Silland CS, Penner TL, Williams DJ, Mukamel SJ. J Phys Chem 1992;96:2810.
[10] Fujimoto Y, Ozaki Y, Takayanagi M, Nakata M, Iriyama K. J Chem Soc Faraday Trans 1996;92:431.
[11] Königstein C, Neumann-Spallart M, Bauer R. Electrochim Acta 1998;43:2435.
[12] Zhai J, Gan LB, Huang CH. Applied Surface Sci 1999; 140:223.
[13] Sahay AK, Mishra BK, Behera GB, Shah DO. Ind J Chem A 1988;27:561.
[14] Newkome GR, Mishra A, Moorefield CN. J Org Chem 2002;67:3957.
[15] Mishra A, Behera RK, Behera GB. Ind J Chem B 2000; 39:783.
[16] Kamlet MJ, Abboud JLM, Taft RW. Prog Phys Org Chem 1981;13:485.
[17] Lopez AT, Lopez AF, Tapia EMJ, Lopez AI. J Phys Chem 1993;97:4704.
[18] Lopez AT, Lopez AF, Tapia EMJ, Lopez AI. J Lumin 1994;59:369.
[19] Al-Ansari IAZ. Bull Soc Chim Fr 1997;134:593.
[20] Lenhard JR, Cameron AD. J Phys Chem 1993;97:4916.
[21] Buston JEH, Marken F, Anderson HL. Chem Commun 2001:1046.
[22] Galus Z. Fundamentals of electrochemical analysis. 2nd ed. Warsaw: Polish Scientific Publishers PWN; 1994.
[23] Gosser DK. Cyclic voltammetry simulation and analysis of reaction mechanisms. New York: Wiley-VCH; 1993.
[24] Bard AJ, Faulkner LR. Electrochemical methods. New York: John Wiley & Sons; 1980.
[25] Nicholson RS, Shain I. Anal Chem 1964;36:706.
[26] Since the nature of compounds **11**–**17** was not investigated, their structure is not presented in this work.
[27] Takada K, Díaz DJ, Abruña HD, Cuadrado I, Casado C, Alonso B, Morán M, Losada J. J Am Chem Soc 1997; 119:10763.
[28] Ammar F, Savéant JM. J Electroanal Chem 1973;47:215.
[29] Flanagan JB, Marel S, Bard AJ, Anson FC. J Am Chem Soc 1978;100:4248.
[30] Rudolph M, Reddy DP, Feldberg SW. Anal Chem 1994; 66:589 A.
[31] Godínez LA, Patel S, Criss CM, Kaifer AE. J Phys Chem 1995;99:17449.